Fan *et al.*
Protection and Control of Modern Power Systems (2023) 8:19
https://doi.org/10.1186/s41601-023-00295-w

Protection and Control of Modern Power Systems

ORIGINAL RESEARCH

Open Access

Three-stage day-ahead scheduling strategy for regional thermostatically controlled load aggregators

Dejin Fan[1], Shu Zhang[1*], He Huang[1], Liping Zhou[1], Yang Wang[1] and Xianyong Xiao[1]

Abstract

Thermostatically controlled loads (TCLs) are regarded as having potential to participate in power grid regulation. This paper proposes a scheduling strategy with three-stage optimization for regional aggregators jointly participating in day-ahead scheduling to support demand response. The first stage is on the profit of aggregators and peak load of the grid. The line loss and voltage deviation of regulation are considered to ensure stable operation of the power grid at the second stage, which guarantees the fairness of the regulation and the comfort of users. A single temperature adjustment strategy is used to control TCLs to maximize the response potential in the third stage. Finally, digital simulation based on the IEEE 33-bus distribution network system proves that the proposed three-stage scheduling strategy can keep the voltage deviation within ± 5% in different situations. In addition, the Gini coefficient of distribution increases by 20% and the predicted percentage of dissatisfied is 48% lower than those without distribution.

Keywords Demand response, Thermostatically controlled loads, Three-stages scheduling strategy, Regional aggregators, PPD, Gini coefficient

1 Introduction

Renewable energy (RE) will be the main energy source in the future because of its green and renewable characteristics. However, with the development of RE, its own characteristics of randomness and intermittence [1] make the scheduling of the system difficult. To increase the flexibility of the traditional scheduling model, a trend that the system considers the demand side as partially controllable is inevitable. Thermostatically controlled loads (TCLs), such as air conditioning loads, heat pumps, electric water heaters, and refrigerators, can serve as indispensable demand response (DR) [2–4] resources, and can be progressively used to address RE variability quickly, economically and effectively [5].

*Correspondence:
Shu Zhang
zs20061621@163.com
[1] College of Electricial Engineering, Sichuan University, Chengdu, Sichuan, China

Using the adjustability of TCLs to regulate the variability of renewable energy resources has important practical significance for the power grid [6–8]. The main purpose of TCLs participating in power grid regulation is to solve the consumption problem. Reference [9] uses maximum power tracking control to control TCLs in real time, realizes household photovoltaic consumption, and promotes the development of household distributed energy resource technology. A real-time zero-energy potential evaluation method with the adoption of TCTR for PVACs is proposed to balance the PV generation and ACs in [10], while through the benefit-driven approach, the optimal scheduling of distributed energy resources and flexible TCLs are realized in [11]. While the above only consider the situation in which RE generation is more than loads, RE often cannot fully meet the load demand and the participation of the power grid is also needed to ensure the balance between the supply and demand of regional power when RE is being completely used.

On the demand side, the concept of aggregator is often used to represent the aggregated loads participating in power grid regulation. TCL adjustability is often used for grid frequency regulation [12, 13], and a voltage regulation strategy is proposed in [7], one which uses the adjustability of TCLs to ensure the voltage stability of the power grid. Aggregated TCLs can also be used to realize the optimal allocation of power grid regulation tasks [14–23]. TCLs are used to participate in day-ahead dispatch [21–23], while a day-ahead scheduling strategy with TCLs is proposed to achieve peak load shedding [24]. A hierarchical control strategy for TCLs is proposed to meet the scheduling requirements, ensure user comfort and reduce communication requirements in [16]. A two-stage strategy is proposed to optimally dispatch the adjustable quantity provided by TCLs in [14], with the lower stage adopting the active control strategy and the upper stage establishing the energy exchange market. A real-time local electricity market for heating, ventilation, and air conditioning loads (HVACs) considering multiple distributed energy resources (DERs) is proposed in [19]. However, the application of the market mechanism will result in some aggregators not obtaining the allocated amount when there is a small number of aggregators. This will lower the enthusiasm of aggregators to participate in regulation. Furthermore, when the loads of aggregators have a certain spatial concentration, regional regulation will have a certain impact on the safe and stable operation of the power grid.

For the fairness of scheduling, and ensuring the comfort of users and reducing the impact of regulation on the grid operation, this paper proposes a three-stage scheduling strategy of regional aggregators of TCLs jointly participating in day-ahead scheduling. The main contributions of this paper are as follows:

Firstly, a three-stage framework is proposed for TCLs, in which the TCLs are scheduled at grid, aggregator and load levels by regulating TCLs in a distributed manner. At the first stage, an electric power transaction is built for aggregated TCLs in which the total regulation is obtained when aggregators can get the maximum interest and the peak load is at the minimum. The second stage is a distribution regulation among aggregators where the change of grid operation caused by regulations is considered, and an optimal adjustment strategy is then proposed to control the aggregated TCLs to achieve the regulation objective at the third stage. Each aggregator can get regulation and interest from power system operation. The fairness of adjustment can be ensured because of the spatial distribution of TCL aggregators in the distribution network. The three-stage scheduling strategy proposed in this paper has better performance in the interests of aggregators and peak load in voltage constraint than the two-stage strategy.

Secondly, a single temperature adjustment strategy is proposed to control TCLs in the three-stage day-ahead scheduling strategy. The temperature change of each user with heterogeneous TCL can be calculated. Because of the different initial setting temperatures, load parameters and space environments, the single temperature adjustment strategy for each TCL has advantages in the comfort level compared to group adjustment. Based on the single temperature adjustment strategy, a subsidy settlement method considering the adjustment contribution of each user is proposed in the paper.

In the following, the framework of the three-stage scheduling is introduced in Sect. 2. The regulatory capacity of the TCL aggregator is described in Sect. 3, and the three-stage optimization model of the strategy is explained in Sect. 4. Section 5 is the case study based on the IEEE 33-bus distribution power system, and the conclusion is presented in Sect. 6.

2 Framework of three-stage schedule

In a smart grid, the load data of the users can be obtained by advanced metering infrastructure (AMI) in real-time. Users can control their appliances with their phones using the Smart Home Cloud Platform (SHCP). Accordingly, it is possible for loads to participate in demand response with the grid and RE. The framework is a three-stage optimization strategy proposed in this paper.

(1) In the first stage, the distributed aggregators (DAGGs) determine the adjustable range (AR) of loads within the jurisdiction and report it to the total aggregator (TAGG) which is not real and only used to represent DAGGs to participate in regulation. TAGG participates in day-ahead scheduling with grid and RE under the condition that the peak of the electricity is at a minimum, the interests of the aggregator are the largest, and the total regulations of each time are obtained.
(2) In the second stage, because of the different spatial distributions of aggregators, TAGG obtains the regulation quantity (RQ) of each DAGG when the power grid loss is at a minimum, and the voltage deviation is in the allowable range.
(3) In the third stage, DAGG obtains the specific temperature change (TC) of each load with the best user comfort and sends the TC of each load to the users. The users regulate their TCLs with a new temperature setpoint (NTS) through the SHCP. Finally, the adjustment results (ARS) are sent to DAGGs by AMI (Fig. 1).

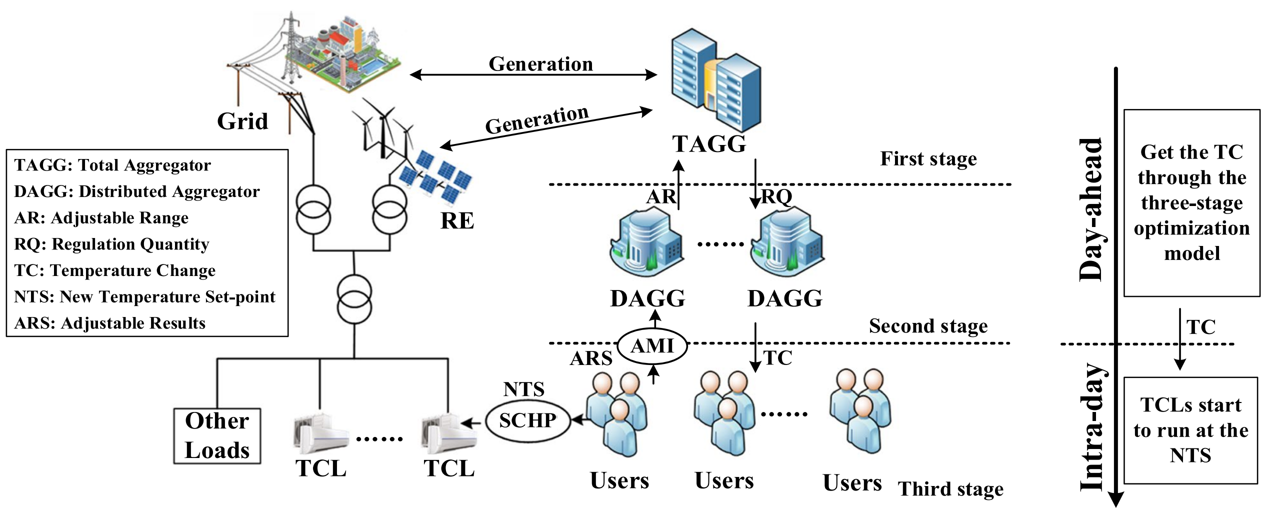

Fig. 1 Framework of three-stage schedule

3 Regulatory capacity of TCL aggregator

In many studies, the virtual energy storage [7, 14], high-dimensional [8], capacitance resistance [25], thermal inertia [24] and black box models [26] have been used to represent TCLs. For a single TCL, the model is always described by an equivalent thermal parameter (ETP) model [27, 28], and the indoor temperature and the building wall temperature can be written as:

$$\begin{aligned}\dot{T}_i(t) &= \frac{dT_i(t)}{dt} \\ &= -\frac{1}{C_a}\left(\frac{1}{R_2}+\frac{1}{R_1}\right)T_i(t)+\frac{1}{C_aR_1}T_m(t) \\ &\quad+\frac{1}{C_a}\left(\frac{T_o(t)}{R_2}+Q(t)\right)\end{aligned} \tag{1}$$

$$\dot{T}_m(t)=\frac{dT_m(t)}{dt}=\frac{1}{C_mR_1}T_i(t)-\frac{1}{C_mR_1}T_m(t) \tag{2}$$

where T_i, T_m and T_o represent the indoor temperature, building wall temperature and outdoor temperature, respectively. R_1 and R_2 are the equivalent thermal resistances between indoor air and outdoor, indoor air and wall, respectively. C_a and C_m are the respective equivalent heat capacities of the indoor and the wall, and Q is the heat exchange capacity of TCL. $s(t)$ indicates the start and stop of the TCL, and is calculated as:

$$s(t+1)=\begin{cases}1, & T_i(t+1)>T_{set}+\delta \\ 0 & T_i(t+1)<T_{set}-\delta \\ s(t) & otherwise\end{cases} \tag{3}$$

where T_{set} is the set temperature of the TCL and δ represents the temperature dead zone. Ignoring the wall parameters, the expression of the indoor temperature is simplified as:

$$T_i(t+1)=T_o(t+1)-(T_o(t+1)-T_i(t))e^{-1/R_1C_a} \tag{4}$$

$$T_i(t+1)=T_o(t+1)-QR_1-(T_o(t+1)-QR_1-T_i(t))e^{-1/R_1C_a} \tag{5}$$

$$P=\frac{Q}{\eta}$$

where η represents the energy efficiency ratio, and P is the electric power of the TCL. The values of P can be calculated as:

$$P=\begin{cases}P_{rated} & s(t)=1 \\ 0 & s(t)=0\end{cases} \tag{6}$$

Since the TCL generally works through the compressor, when the load is turned on, the electric power is the rated electric power, and when the load is turned off, the electric power is 0.

Although the adjustable potential of a single TCL is limited, aggregating TCLs can provide great regulation potential for the power grid because of the large scale and large number of TCLs. The sum of the electric power for all TCLs at t is given as:

$$P_{agg}=\sum_{i=1}^{N}P_i=\sum_{i=1}^{N}s(i)\cdot P_{rated} \tag{7}$$

where P_i is the electric power of TCL i, and $s(i)$ represents the on–off state of the TCL i, which is related to the setting temperature of the TCL. Therefore, the power model of the aggregator can be represented by a function with T_{set}, as:

$$P_{aggi} = P_{aggi}(R_1, C_a, T_o, T_{set}) \tag{8}$$

When the maximum setting temperature change is ΔT, the power of the aggregator can be described as:

$$P_{aggi} = P_{aggi}(R_1, C_a, T_o, T_{set} + \Delta T) \tag{9}$$

Then, the maximum adjustment capacity of the aggregator can be expressed as:

$$P_{d\,\max,aggi} = P_{aggi}(R_1, C_a, T_o, T_{set}) - P_{aggi}(R_1, C_a, T_o, T_{set} + \Delta T) \tag{10}$$

The minimum adjustment capacity should be 0. Therefore, the adjustment range of the aggregator can be represented as:

$$\begin{aligned}&\left[P_{d\,\min,aggi}, P_{d\,\max,aggi}\right] \\ &= \left[0, P_{aggi}(R_1, C_a, T_o, T_{set})\right. \\ &\quad \left.-P_{aggi}(R_1, C_a, T_o, T_{set} + \Delta T)\right]\end{aligned} \tag{11}$$

Each DAGG calculates the adjustable interval according to the user load parameters and preferences in the jurisdiction area and sends the information to TAGG to participate in the day ahead optimal scheduling.

4 Three-stage optimization model of strategy

Based on the framework of the three-stage schedule, a three-stage optimization model is built. Figure 2 shows its overall flowchart. As can be seen, the first stage calculates the total adjustment amount by a multi-objective genetic algorithm (NSGA-II) when the peak load is at a minimum and the aggregator interest is at its maximum. The second stage distributes regulation to each aggregator when the voltage constraint is satisfied and the line loss is at a minimum, while the third stage is to calculate temperature change when the predicted percentage of dissatisfied (PPD) is at a minimum. PSO is used to solve the optimization problem in the second and third stages.

4.1 The first stage

In the first stage, an electric power transaction is built, and the minimum peak load of the power grid after TCL regulation is taken as the optimization goal to ensure the safe and stable operation of the power grid, expressed as:

$$\min(\max(P_{base,i} + P_{ac,i})) \tag{12}$$

where $P_{base,\,i}$ represents the power of other loads, and $P_{ac,\,i}$ represents the power of TCLs at time i. The power constraint is shown as:

$$P_{base,i} + P_{ac,i} = P_{grid,i} + P_{newpower,i} \tag{13}$$

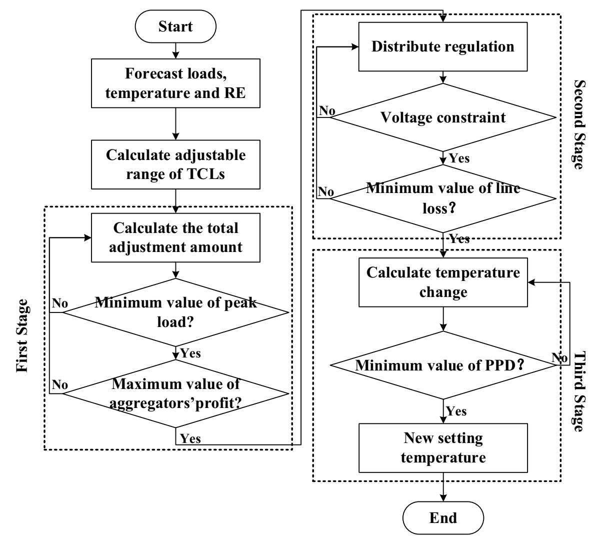

Fig. 2 Overall flowchart of the optimization model

The second goal of the first stage is to obtain the greatest benefit for the TCL aggregators. According to [29], the electricity price of demand response electricity is the real-time electricity price of the demand side response market, which has a linear relationship with the total load, as:

$$Ep_{dr} = aP_{all} + b \tag{14}$$

where Ep_{dr} represents the real-time electricity price of the demand side market over a certain period of time, P_{all} represents the total load in the network at this time, while a and b represent positive electricity price coefficients. The subsidy of the aggregator to users is a quadratic function of the demand side response reduction, given as:

$$B = k \cdot P_{dr}^2 = k(L_{before} - L)^2 \tag{15}$$

$$L = L_{base} + L_{ac} \tag{16}$$

where B represents the total subsidy given to users by the aggregator, k is the subsidy cost coefficient of the aggregator to users, and P_{dr} represents the demand side response at this time. L_{before} and L represent the total load before and after the demand side response, respectively. L_{base} represents the basic load of the power grid, and L_{ac} represents TCLs' power.

From (14) and (15), the optimization objective function can be described as:

$$\max G = \max\left(\sum_{t=t_1}^{t_2}\left(aP_{all,t} + b\right) \cdot P_{dr,t} - \sum_{t=t_1}^{t_2} k \cdot P_{dr,t}^2\right) \tag{17}$$

where t_1 and t_2 are the respective start and end times of using TCLs. The inequality constraint should be considered, i.e.:

$$P_{dr,t,\min} \leq P_{dr,t} \leq P_{dr,t,\max} \tag{18}$$

where $P_{dr,\,t,\,min}$ and $P_{dr,\,t,\,max}$ are the minimum and maximum adjustable capacities of the aggregator at a certain time, respectively.

Finally, because of the advantages of fast running speed and good convergence of solution sets, the multi-objective genetic algorithm NSGA-II [30] is used to solve the double objective optimization model, and the adjustment amount, total benefit and total user subsidy are obtained.

4.2 The second stage

After obtaining the adjustment amount of the total aggregator, the next step is to allocate the adjustment amount to each aggregator. The TCLs that can be regulated by each aggregator have certain spatial differences, so the impact of regulation behavior on power grid operation should be fully considered during distribution. For branch connecting points m and n, the power flow is calculated as:

$$v_m - v_n = 2(r_{mn}P_{mn} + x_{mn}Q_{mn}) - (r_{mn}^2 + x_{mn}^2)l_{mn} \tag{19}$$

$$l_{mn}v_{mn} = P_{mn}^2 + Q_{mn}^2, l_{mn} \geq 0 \tag{20}$$

where v_m and v_n represent the respective squares of the voltage amplitudes of nodes m and n, r_{mn} and x_{mn} are the respective resistance and reactance of line m–n, while P_{mn} and Q_{mn} represent the active power and reactive power on node m, respectively. l_{mn} is the square of the current amplitude of line m–n.

The grid total line loss P_{loss} can be expressed as:

$$P_{loss} = \sum_{i=1}^{n(i\neq j)} \sum_{j=1}^{n(i\neq j)} l_{ij}x_{ij} \tag{21}$$

The optimization objective function of this stage can be described as:

$$\min P_{loss} = \min \left(\sum_{i=1}^{n(i\neq j)} \sum_{j=1}^{n(i\neq j)} l_{ij}x_{ij} \right) \tag{22}$$

The node voltage deviation constraint is shown as:

$$-5\% \leq vdiff_i = \frac{v_{i,t} - v_{i,o}}{v_{i,o}} \times 100\% \leq 5\% \tag{23}$$

where $vdiff_i$ represents the percentage voltage difference before and after adjustment of the i^{th} node, while $v_{i,\,t}$ and $v_{i,\,o}$ represent the voltages of node i after and before adjustment, respectively. Finally, the multidimensional particle swarm optimization (PSO) algorithm [31] is used to obtain the adjustment of each aggregator at each time because the solution variables are multidimensional.

4.3 The third stage

In terms of controlling TCLs under the jurisdiction of a single aggregator, an optimal adjustment strategy is proposed. From the user perspective, the optimization focus is on the comfort of users. The Fanger thermal comfort model is a common model used to quantify the discomfort of the user and describe the dissatisfaction of the user with room temperature. Since the discomfort is related mainly to the indoor temperature, other factors are assumed to be constants, and then the interpolation method is used to fit the discomfort level of the user and setting temperature. The fitted expression is simplified as [32]:

$$PPD = a(T_{set}^k - T_{set}^0)^2 \tag{24}$$

where the predicted percentage of dissatisfied (PPD) represents the dissatisfaction of the user with the indoor temperature, a is a positive proportional coefficient, the temperature setting value after adjustment is *Tk set*, and *T0 set* represents the expected temperature value of the user, which is the initial TCL setting value. Therefore, the discomfort level of a single user χ is expressed as:

$$\chi = (T_{set}^k - T_{set}^0)^2 \tag{25}$$

Users have different expected temperatures, resulting in different discomfort levels at the same temperature. Therefore, the discomfort level of each user needs to be calculated separately, and the user adjustment behavior also needs to be calculated separately. The optimization goal at the user level is that the overall discomfort level of users is the lowest, which is expressed as:

$$\min \sum \chi = \min \sum (T_{set}^k - T_{set}^0)^2 \tag{26}$$

The temperature constraint is shown as [28, 33]:

$$0 \leq T_{set}^k - T_{set}^0 \leq 3 \tag{27}$$

In the previous content, the influence of temperature regulation on the aggregate power of TCL was analyzed. Therefore, it is also necessary to consider the aggregated power constraint of TCL during optimizing after the change in the temperature setting value.

Because the TCLs under the jurisdiction of the aggregator are heterogeneous, the fitting rate between the daily load curves after the temperature setting value is changed, and the upper optimal daily load curve is taken as the power constraint of the user level optimization model. The curve fitting rate R_{new} in this paper is greater than 0.9, i.e.:

$$R_{new} \geq 0.9 \tag{28}$$

and the fitting rate calculation is given as [36]:

$$R_{new} = 1 - \sqrt{\frac{\sum (y_{1,t} - y_t)^2}{\sum y_t^2}} \tag{29}$$

where $y_{i,\,t}$ and y_t represent the actual and target values at time t, respectively.

Because of the diversity of user regulation behavior, the current set temperature regulation of TCLs is an integer, and the specific temperature regulation of each user needs to be obtained. Therefore, integer programming based on the PSO [31] algorithm is introduced to solve the user-level optimization model. The particle position update formula of PSO is given as:

$$x(t+1) = \begin{cases} x(t) + 1 & g(t+1) > 0 \\ x(t) - 1 & g(t+1) < 0 \\ x(t) + sig(c) & g(t+1) = 0 \end{cases} \tag{30}$$

where $g(t)$ is the direction vector of the particle.

After obtaining the temperature regulation, how to get the subsidies of users becomes a new problem. For user i under the jurisdiction of an aggregator, this paper takes the average adjustment amount of N users with the same user preference and load at each time under each temperature adjustment amount as the contribution of the user under the corresponding temperature adjustment amount [37], expressed as:

$$u_i = P_{agg,N}(R_1, C_a, T_o, T_{set}) - P_{agg,N}(R_1, C_a, T_o, T_{set} + T_r) \tag{31}$$

where u_i is the contribution of user i, T_r is the temperature regulation, and N is 1000 in this paper. Then, the subsidy of user i can be expressed as:

$$C_{users,i} = \frac{u_i}{\sum_{i=1}^{m} u_i} C_{users,sum,r} \tag{32}$$

where $C_{users,\,i}$ is the subsidy of user i, m is the quantity of users, and $C_{users,\,sum,\,r}$ is the sum subsidy of DAGGs.

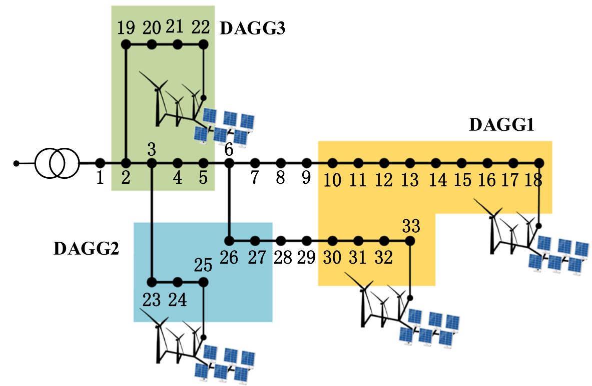

Fig. 3 Spatial distributions of DAGGs in the IEEE 33 nodes

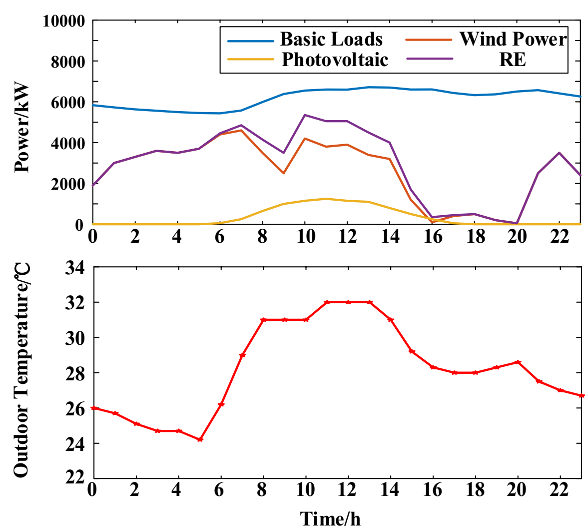

Fig. 4 Prediction of RE, basic loads, and temperature

5 Case studies

Based on the IEEE 33-bus distribution network system, RE and three aggregators are assumed to be in the areas that have different jurisdictions, as shown in Fig. 3. The prediction of RE generation and basic loads of the load regulation point excluding the TCL and the outdoor temperature change are shown in Fig. 4. The 1000 TCLs that are mostly air conditioning loads are assumed to be involved in the regulation of each DAGG, and the load parameters meet the distribution shown in Table 1.

Using Monte Carlo simulation, 1000 groups of load parameters under each aggregator are obtained. Then, TAGG uses the maximum regulation capacity of each aggregator to participate in the day-ahead scheduling.

Table 1 Load Parameters

Parameters	Aggregator		
	DAGG1	DAGG2	DAGG3
T_{set} (℃)	N (22.5, 2.25^2), (15.25)	N (22.5, 2.25^2), (20, 25)	N (22.5, 2.25^2), (20, 22.5)
δ (℃)	N (0.3, 0.03^2), (0.25, 1)	N (0.3, 0.03^2), (0.25, 0.35)	N (0.3, 0.03^2), (0.3, 0.5)
P_{rated} (kW)	N (14, 1.4^2), (10, 18)	N (5.6, 0.56^2), (4.5, 7)	N (14, 1.4^2), (6, 14)
R (℃/kW)	N (2, 0.2^2), (1.5, 2.5)	N (2, 0.2^2), (1.8, 2.2)	2
C_a (kWh/℃)	N (2, 0.2^2), (1.5, 2.5)	N (2, 0.2^2), (1.8, 2.2)	2
η	2.5	2.5	2.5

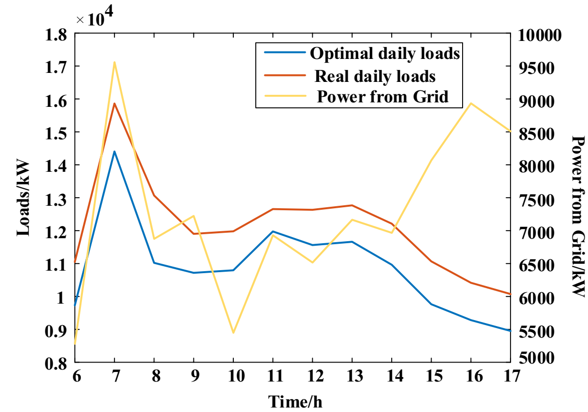

Fig. 5 Power from grid and loads

The coefficients a and b in (14) are 8.25×10^{-5} and 0.2 in this paper, while k is 0.00045 CNY¥/kW^2 [23].

5.1 DAGG with different control points

For the three-stage scheduling strategy shown in Sect. 4, the simulation results of the three-stage optimization model are shown in Table 2. First, the power from the grid and optimal daily loads can be obtained by solving the optimization model of the first stage, as shown in Fig. 5, where the "gamultiobj" function in Matlab is employed to implement NSGA-II.

The peak load of the optimal daily load curve is 14406.061 kW, and the aggregators provide 1457.283 kW peak shaving capacity for the power grid, leading to a saving of 12,241 kWh electricity. The benefit obtained by the aggregators is CNY¥ 7588.988, and the user subsidy is CNY¥ 11,386.5128. At this time, the total power regulations of the aggregators are shown in Table 2.

Different locations of TCL control points can lead to different results in the second stage. While the different results indicate the small difference of adjustment values, the change trend of regulation of each DAGG is the same. In this section, case 1 and case 2 with different control points are employed to study the effectiveness of the proposed strategy. The TCL control points of each DAGG are shown in Table 2. Then, the best regulation of each DAGG is obtained in Table 2 by a 3×12 dimensions PSO algorithm while the outputs are lower than the

Table 2 The results of the three-stage optimization model in different situations

Time	Total power regulation/kW	Regulation in Case 1			Regulation in Case 2		
		DAGG1/kW (Points: 10, 15, 17, 31, 32)	DAGG2/kW (Points: 23, 24, 26)	DAGG3/kW (Points: 4, 5, 19, 20)	DAGG1/kW (Points: 11, 12, 13, 14)	DAGG2/kW (Points: 23, 24, 25, 26)	DAGG3/kW (Points: 19, 20, 21)
6:00	1321.582	802.5116	331.3872	187.6828	774.5307	222.1977	324.8532
7:00	1457.283	692.5997	549.6249	215.0582	433.4235	460.9172	562.9421
8:00	2046.038	494.8865	931.5304	619.6210	524.8299	743.7738	777.4343
9:00	1181.328	387.7899	462.1885	331.3496	392.8116	450.9610	337.5553
10:00	1183.153	392.5036	390.4066	400.2430	402.0373	387.2477	393.8682
11:00	680.548	274.2875	271.8800	134.3801	351.6104	199.5735	129.3638
12:00	1071.073	389.7445	323.0090	358.3191	389.1078	349.2564	332.7084
13:00	1105.788	370.2248	385.7683	349.7953	382.3693	368.0969	355.3222
14:00	1248.646	406.5722	422.9994	419.0745	405.0483	423.7329	419.8649
15:00	1299.580	460.3463	443.6260	395.6081	470.3374	413.5138	415.7292
16:00	1136.680	337.3681	432.4150	366.8965	333.0938	431.8370	371.7487
17:00	1118.818	382.8485	409.2813	326.6882	378.5512	393.5508	346.7160
Fitting ratio		0.9124	0.9008	0.9149	0.9349	0.9382	0.9246
Discomfort level		2363	2622	2280	2502	2572	2557

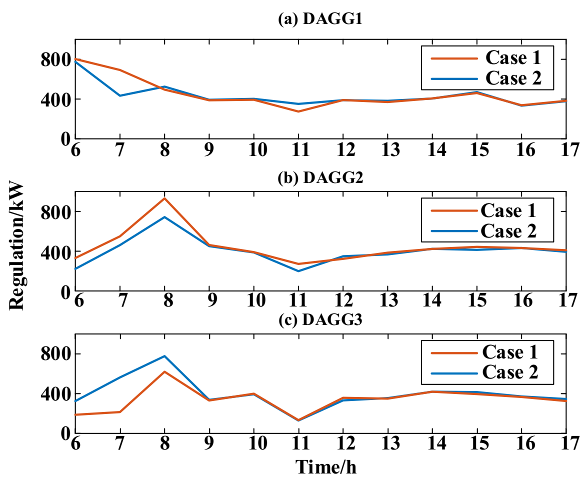

Fig. 6 TCL regulation of each DAGG

regulatory capacity of each TCLs aggregators when the optimal operation of the grid is considered.

Comparing the regulations of case 1 and case 2, as shown in Fig. 6, the regulations have differences from 6:00 to 8:00 because of the volatility of TCLs when opening, but are almost the same at the other times, suggesting that the proposed three-stage scheduling strategy can be used in different situations.

After obtaining the adjustment amount of each DAGG, the TCL temperature setting value is changed to take the best user comfort level as the optimization goal, and the PSO integer programming algorithm is used to optimize the solution, which has 1×1000 dimensions outputs between 0 and 3.

The temperature regulations are obtained by the optimization of the third stage. Taking DAGG1 in case 1 as an example, as shown in Fig. 7, each TCL has different regulations to ensure the thermal comfort level.

In cases 1 and 2, the three-stage scheduling strategy can successfully complete the optimal scheduling, ensure the stable operation of the power grid and reduce the impact on user comfort. In general, the three-stage scheduling strategy proposed is suitable for regional aggregators with different TCL control points.

However, from the TCL power curve in case 1, there are errors caused by the heterogeneity of TCLs. The errors can be reduced by using the battery configured by each DAGG in Fig. 8.

Because this paper studies TCL participation in day-ahead scheduling and the use of a battery as the supplement of TCLs, the mainly affected battery characteristics are the rated power and capacity. Assuming that the price of battery output is 0.2 CNY¥/kWh, the interests of each DAGG are shown in Table 3. DAGGs can obviously receive more interest with battery participation, and the sum subsidy of users is now CNY¥ 10,720.9852.

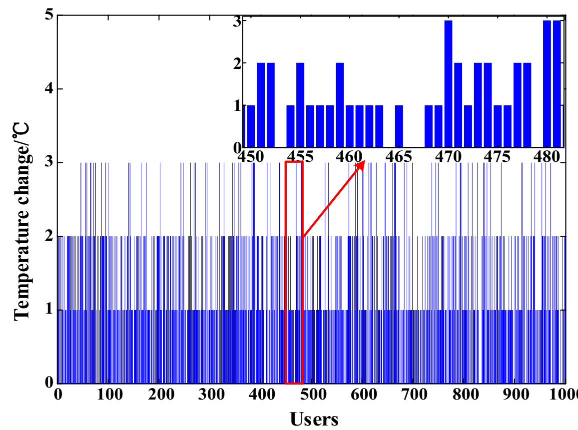

Fig. 7 Temperature change of users of DAGG1

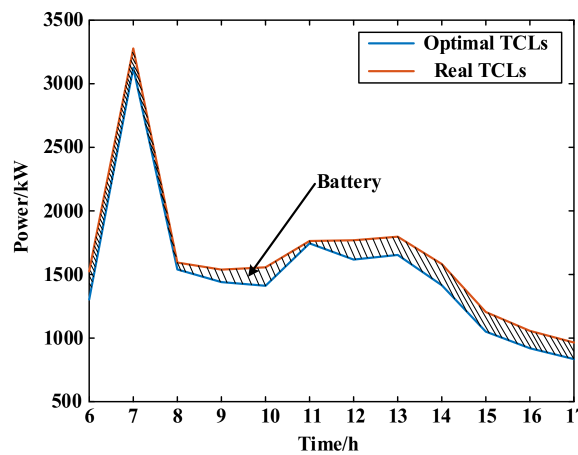

Fig. 8 Battery reducing the errors of TCLs

Table 3 Interest of each DAGG

Interests	DAGG1	DAGG2	DAGG3
From regulation/yuan	2671.9539	2774.8340	2142.2001
From battery/yuan	279.8827	276.6066	109.0383
Sum/yuan	2951.8366	3051.4406	2251.2384

5.2 Comparison with the two-stage scheduling strategy without distribution function

A. The two-stage scheduling strategy with market

In the three-stage scheduling strategy proposed in this paper, the second stage is to distribute the regulation to aggregators to ensure the fairness of regulation. This section compares the results of the three-stage scheduling with distribution and two-stage scheduling without distribution [6, 14, 24].

The Gini coefficient is an indicator that measures the inequality of income distribution and is used to measure the fairness of the distribution process of regulation in this paper. The closer its value is to 0, the more even the distribution is [34]. The Gini coefficient is calculated as:

$$G = \frac{\sum_{i=1}^{n}\sum_{j=1}^{n}\left|x_i - x_j\right|}{2n\sum_{i=1}^{n}x_i} \tag{33}$$

where G is the Gini coefficient, n is the number of all members, and x_i is the data of member i.

Assuming that the regulated electricity price relationship of each DAGG is as shown in Fig. 9, the second stage in the scheduling strategy proposed in this paper is replaced by the market form. After optimal dispatching, the voltage deviations of each node of the IEEE 33-bus distribution power system with or without a market are shown in Fig. 10. As shown, the voltage deviations of nodes 15–18 are larger than the largest deviation using the two-stage strategy. When using the two-stage strategy, the discomfort of the users of each DAGG is 9000, 2686 and 2331, respectively, and these levels are significantly higher than the discomfort of the users of each DAGG in the proposed strategy.

Using (33) to calculate the Gini coefficient of the two strategies, the Gini coefficients are 0.3510 and 0.5444 with and without distribution, respectively. Thus, it proves that using the three-stage scheduling strategy proposed in this paper is clearly safer for the grid, more comfortable for users and fairer for DAGGs.

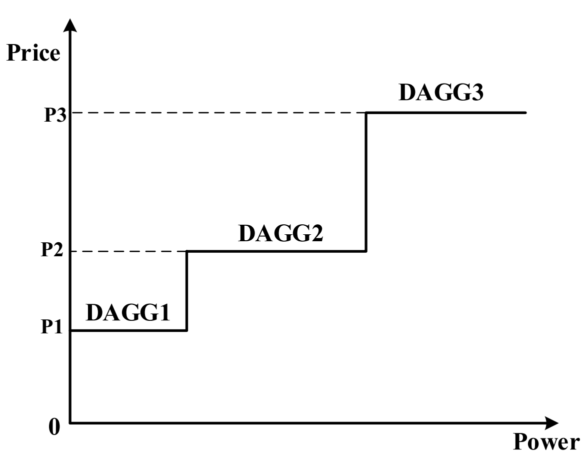

Fig. 9 Regulated electricity price relationship of DAGGs

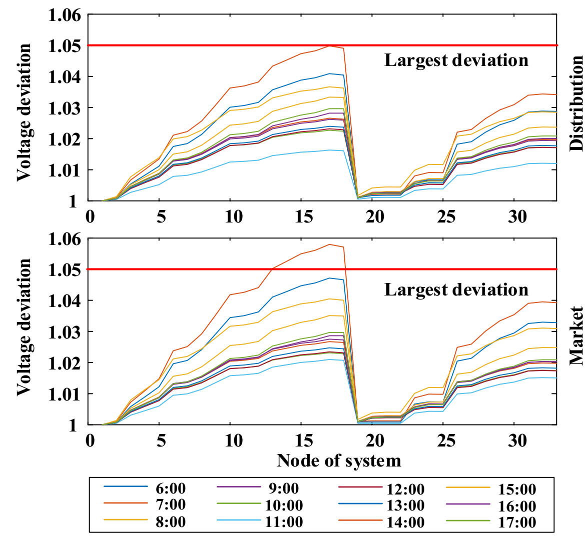

Fig. 10 Voltage deviations with distribution or market

B. The two-stage scheduling strategy with voltage constraint

The results are compared with the two-stage scheduling strategy with voltage constraint, which combines the first and second stages proposed in this paper into one stage. After solving the multi-objective optimization model of each first stage, the Pareto front of each strategy is shown in Fig. 11. It is clear that the peak load is lower and the total interest is greater with the three-stage strategy proposed here.

Thus, the three-stage scheduling strategy proposed can obtain the greater interest for aggregators and better user comfort level when the safe and stable operation of power grid is guaranteed.

5.3 Comparison with the scheduling strategy based on group adjustment

Single control is used to control TCLs of aggregators in this paper, and every TCL gets its own temperature change because of the different parameters. Group control has always been used to control TCLs [17, 35]. When compared with the group control where grouping is based on rating power, as shown in Table 4, the single control can get lower PPD, which can better ensure user comfort.

In the third stage, the different temperature regulations of each TCL are calculated in the final stage, and are used as a basis for subsidy allocation. However, for users with the same temperature change, the different setting

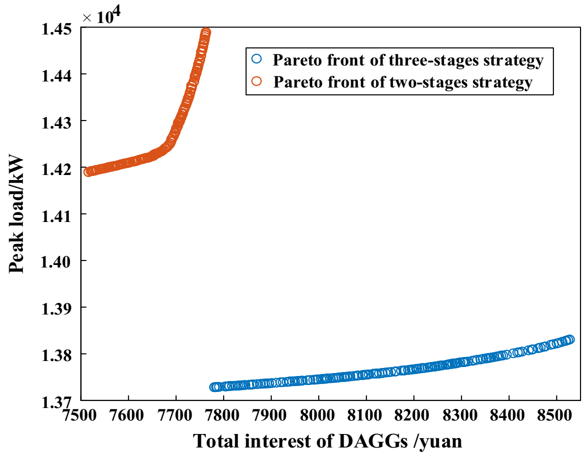

Fig. 11 Pareto front of different strategy

Table 4 PPD with different control mode

Loads control mode	Single control	Group control (5 groups)	Group control (3 groups)
PPD	2502	3033	6840

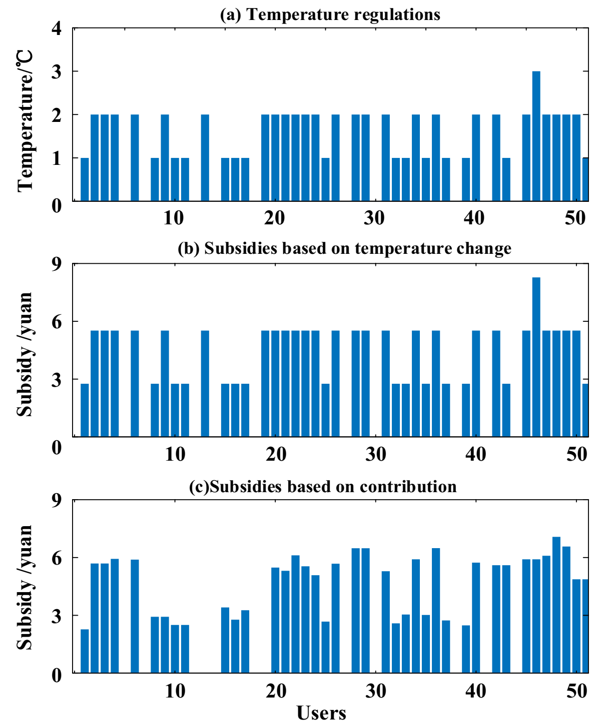

Fig. 12 Temperature change and subsidies of DAGG1

temperatures and space environments should lead to different contributions in the regulation, resulting in different subsidies. In Fig. 12, taking 50 users of DAGG1 in case 1 as an example, users having the same temperature regulations can receive different subsidies because of the TCLs' heterogeneity and setting-temperature difference.

6 Conclusions

A three-stage day-ahead scheduling strategy is proposed for TCLs. This scheduling strategy adds a distribution function among the regional load aggregators to ensure the stable operation of the power grid, guarantee the fairness of regulation among aggregators and improve user comfort. Furthermore, because of the heterogeneity of TCLs, the optimal fitting curve cannot be met entirely in the third stage. Therefore, the scheme in which aggregators configure a certain battery is proposed to reduce error of load scheduling and increase aggregator profit. The effectiveness of the proposed strategy is verified by simulation with the IEEE 33-bus distribution network system.

The results show that the three-stage scheduling strategy proposed in this paper can adapt to different situations with different TCL control points of aggregators. Compared with the two-stage strategy not containing distribution function, the proposed strategy can better ensure the safe and stable operation of the power grid, and keeps the voltage deviation within ± 5%. Simultaneously, the Gini coefficient increases by 20%, and the comfort level of the users increases by 48% in the case study. Compared with the strategy based on group adjustment, the single temperature adjustment used in this paper can better insure user comfort. Given this, the subsidy settlement method considering the adjustment contribution of each user is then proposed.

Acknowledgements
Not applicable

Author contributions
DF is responsible for the main work of writing manuscript. SZ (Corresponding Author) is responsible for the core innovation and revision of paper. HH is responsible for the data analysis of the model in the paper. LZ is responsible for the data analysis of the model in the paper. YW is responsible revising the grammar and other languages of the paper. XX is responsible for the core innovation of the paper. All authors read and approved the final manuscript.

Funding
This work was supported in part by the National Natural Science Foundation of China (No. 52007126 and No. U2166209).

Availability of data and materials
Not applicable.

Declarations

Competing interests
The authors declare that they have no known competing financial interests or personal relationships that could have appeared to influence the work reported in this paper.

Received: 17 October 2022 Accepted: 28 April 2023
Published online: 12 May 2023

References

1. Ding, Y., Xie, D., Hui, H., Xu, Y., et al. (2021). Game-theoretic demand side management of thermostatically controlled loads for smoothing tie-line power of microgrids. *IEEE Transactions on Power Systems, 36*(5), 4089–4101.
2. Chen, Q., Wang, W., & Wang, H. (2022). Bi-level optimization model of an active distribution network based on demand response. *Power System Protection and Control, 50*(16), 1–13.
3. Yang, H., Zhang, X., Ma, Y., et al. (2021). Critical peak rebate strategy and application to demand response. *Protection and Control of Modern Power Systems, 6*(3), 357–370.
4. Ding, X., Xu, J., Sun, Y., et al. (2022). A demand side controller of electrolytic aluminum industrial microgrids considering wind power fluctuations. *Protection and Control of Modern Power Systems, 4*, 751–763.
5. Radaideh, A., Al-Quraan, A., Al-Masri, H., et al. (2021). Rolling horizon control architecture for distributed agents of thermostatically controlled loads enabling long-term grid-level ancillary services. *International Journal of Electrical Power & Energy Systems, 127*, 106630.
6. Wei, C., Xu, J., Liao, S., et al. (2018). Coordination optimization of multiple thermostatically controlled load groups in distribution network with renewable energy. *Applied Energy, 231*, 456–467.
7. Zhang, M., & Bao, Y. (2021). Voltage control strategy for distribution network with thermostatically controlled loads equivalent energy storage model considering minimum-on-off time. *International Journal of Electrical Power & Energy Systems, 133*, 107268.
8. Song, M., Gao, C., Shahidehpour, M., et al. (2019). Multi-time-scale modeling and parameter estimation of TCLs for smoothing out wind power generation variability. *IEEE Transactions on Sustainable Energy, 10*(1), 105–118.
9. Burmester, D., Rayudu, R., & Seah, W. K. G. (2018). Use of maximum power point tracking signal for instantaneous management of thermostatically controlled loads in a DC nano grid. *IEEE Transactions on Smart Grid, 9*(6), 6140–6148.
10. Jiang, T., Ju, P., Wang, C., Li, H., et al. (2021). Coordinated control of air-conditioning loads for system frequency regulation. *IEEE Transactions on Smart Grid, 12*(1), 548–560.
11. Ross, S., & Mathieu, J. (2021). Strategies for network-safe load control with a third-party aggregator and a distribution operator. *IEEE Transactions on Power Systems, 36*(4), 3329–3339.
12. Mendieta, W., & Cañizares, C. A. (2021). Primary frequency control in isolated microgrids using thermostatically controllable loads. *IEEE Transactions on Smart Grid, 12*(1), 93–105.
13. Wang, Z., Bao, Y., & Di, H. (2020). Power system virtual inertia implemented by thermostatically controlled loads. *IET Smart Grid, 3*(4), 530–537. https://doi.org/10.1049/iet-stg.2019.0246
14. Song, M., Sun, W., Wang, Y., et al. (2020). Hierarchical scheduling of aggregated TCL flexibility for transactive energy in power systems. *IEEE Transactions on Smart Grid, 11*(3), 2452–2463.
15. Wei, Q., Liao, Z., Song, R., et al. (2021). Self-learning optimal control for ice-storage air conditioning systems via data-based adaptive dynamic programming. *IEEE Transactions on Industrial Electronics, 68*(4), 3599–3608.
16. Xia, M., Song, Y., & Chen, Q. (2019). Hierarchical control of thermostatically controlled loads oriented smart buildings. *Applied Energy, 254*, 113493. https://doi.org/10.1016/j.apenergy.2019.113493
17. Gong, X., Castillo-Guerra, E., Cardenas-Barrera, J. L., et al. (2021). Robust hierarchical control mechanism for aggregated thermostatically controlled loads. *IEEE Transactions on Smart Grid, 12*(1), 453–467.
18. Li, W., Gong, G., Ren, Z., et al. (2022). A method for energy consumption optimization of air conditioning systems based on load prediction and energy flexibility. *Energy, 243*, 123111.
19. Hui, H., et al. (2022). A transactive energy framework for inverter-based HVAC loads in a real-time local electricity market considering distributed energy resources. *IEEE Transactions on Industrial Informatics, 18*(12), 8409–8421.
20. Li, S., Peng, J., Zou, B., et al. (2021). Zero energy potential of photovoltaic direct-driven air conditioners with considering the load flexibility of air conditioners. *Applied Energy, 304*, 117821.
21. Luo, F., Dong, Z., Meng, K., et al. (2017). An operational planning framework for large-scale thermostatically controlled load dispatch. *IEEE Transactions on Industrial Informatics, 13*(1), 217–227.
22. Chen, P., Bao, Y., Zhu, X., et al. (2019). Day-ahead scheduling of large numbers of thermostatically controlled loads based on equivalent energy storage model. *Journal of Modern Power Systems and Clean Energy, 7*(3), 579–588.
23. Cheng, L., Bao, Y., et al. (2020). A day-ahead scheduling of large-scale thermostatically controlled loads model considering second-order equivalent thermal parameters model. *IEEE Access, 8*, 102321–102334.
24. Chen, Y., Luo, F., Dong, Z., et al. (2019). A day-ahead scheduling framework for thermostatically controlled loads with thermal inertia and thermal comfort model. *Journal of Modern Power Systems and Clean Energy, 7*(3), 568–578.
25. Zhang, R., Jiang, T., Li, G., et al. (2021). Stochastic optimal energy management and pricing for load serving entity with aggregated TCLs of smart buildings: a Stackelberg game approach. *IEEE Transactions on Industrial Informatics, 17*(3), 1821–1830.
26. Kazmi, H., Suykens, J., Balint, A., et al. (2019). Multi-agent reinforcement learning for modeling and control of thermostatically controlled loads. *Applied Energy, 238*, 1022–1035.
27. Wang, P., Wu, D., & Kalsi, K. (2020). Flexibility estimation and control of thermostatically controlled loads with lock time for regulation service. *IEEE Transactions on Smart Grid, 11*(4), 3221–3230.
28. Fan, D., Zhang Shu, S., Wang, Y., et al. (2022). Day ahead scheduling strategy for air conditioning load aggregators considering user regulation behavior diversity. *Power System Protection Control, 50*(17), 133–142.
29. Soliman, H. M., & Leon-Garcia, A. (2014). Game-theoretic demand-side management with storage devices for the future smart grid. *IEEE Transactions on Smart Grid, 5*(3), 1475–1485.
30. Zhou, H., Ding, M., Hu, B. et al. (2018). A NSGA-II based peak load shifting optimization method for customers with distributed generators considering time-of-use price. In *2018 37th Chinese Control Conference* (pp 7626–7631).
31. Sisodiya, S., Kumbhar, G. B., & Alam, M. N. (2018). A home energy management incorporating energy storage systems with utility under demand response using PSO. In: *2018 IEEMA engineer infinite conference* (pp. 1–6).
32. Liu, S. (2019). *Temperature control load control strategy and incentive mechanism for smart grid frequency regulation*. Yanshan University.
33. Huang, Q., & Li, J. (2020). Research progress on the mechanism of human thermal sensation changes when the ambient temperature changes suddenly. *Journal of Textile Research, 41*(04), 188–194.
34. Kendall, M. G., & Stuart, A. (1958). *The advanced theory of statistics*. Hafner Publishing Co.
35. Chu, C., Jong, T., Huang, Y. (2007). Mitigating DLC constraints of air-conditioning loads using a group-DLC method. In *IEEE power engineering society general meeting* (pp. 1–6), FL, USA.
36. Zhang, S. (2002). Discussion on the goodness of fit index of curve regression. *Chinese Health Statistics, 01*, 9–11.
37. Vanouni, M., & Lu, N. (2018). A reward allocation mechanism for thermostatically controlled loads participating in intra-hour ancillary services. *IEEE Transactions on Smart Grid, 9*(5), 4209–4219.